

Design progress of Soft X-ray Beamlines

- ID25 NanoARPES
- ID26 Soft X-ray NanoProbe

Sae Hee Ryu, Siwoo Noh (Korea-4GSR)

Byeong-Gyu Park, Jaeyoon Baik, Ki-jeong Kim (PLS-II)

Yeong Kwan Kim, Young-Sang Yu (KOSUA)

Aaron Bostwick, Timur Kim, Simon Bongjin Mun (MAC)



Soft X-ray beamlines of Korea-4GSR

Beamlines of 1st phase

- ① BioPharma-BioSAXS
- ② Material Structure Analysis
- ③ **Soft X-ray Nano-probe**
- ④ **nanoARPES**
- ⑤ Coherent X-ray Diffraction
- ⑥ Coherent Small-angle X-ray Scattering
- ⑦ Real-time X-ray Absorption Fine Structure
- ⑧ Bio Nano crystallography
- ⑨ High Energy Microscopy
- ⑩ Nanoprobe



Electron Beam Energy: 4 GeV (Approx. 800 m Circular Orbit)

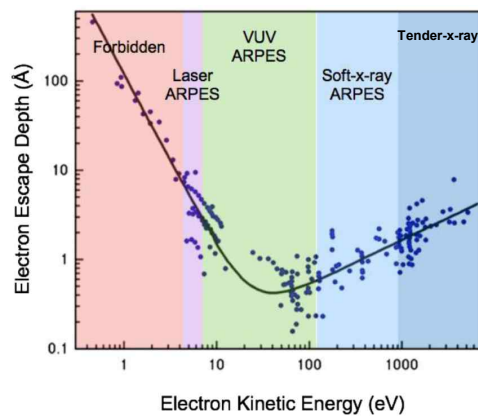
Electron Beam Emittance: ~ 62 pm·rad (PLS-II: 5800 pm·rad)

Beamlines: Over 40 (Initially 10)

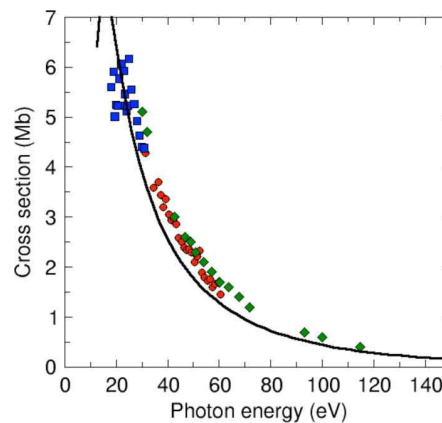
Acceleration Method: Electron Gun, Injector Linac, 4 GeV Booster

Storage Ring: MBA-Based 7BA Magnet Configuration

Soft X-ray beamlines of Korea-4GSR



Surface sensitivity



Elemental cross section

Benefits of Soft X-ray

- ① High sensitivity for light elements
- ② Chemical state sensitivity
- ③ Surface sensitivity
- ④ High energy resolution
- ⑤ High momentum resolution

Applications

Condensed matter

Materials

Chemistry

Magnetism

Biology

ARPES, RIXS

STXM, **XAS**

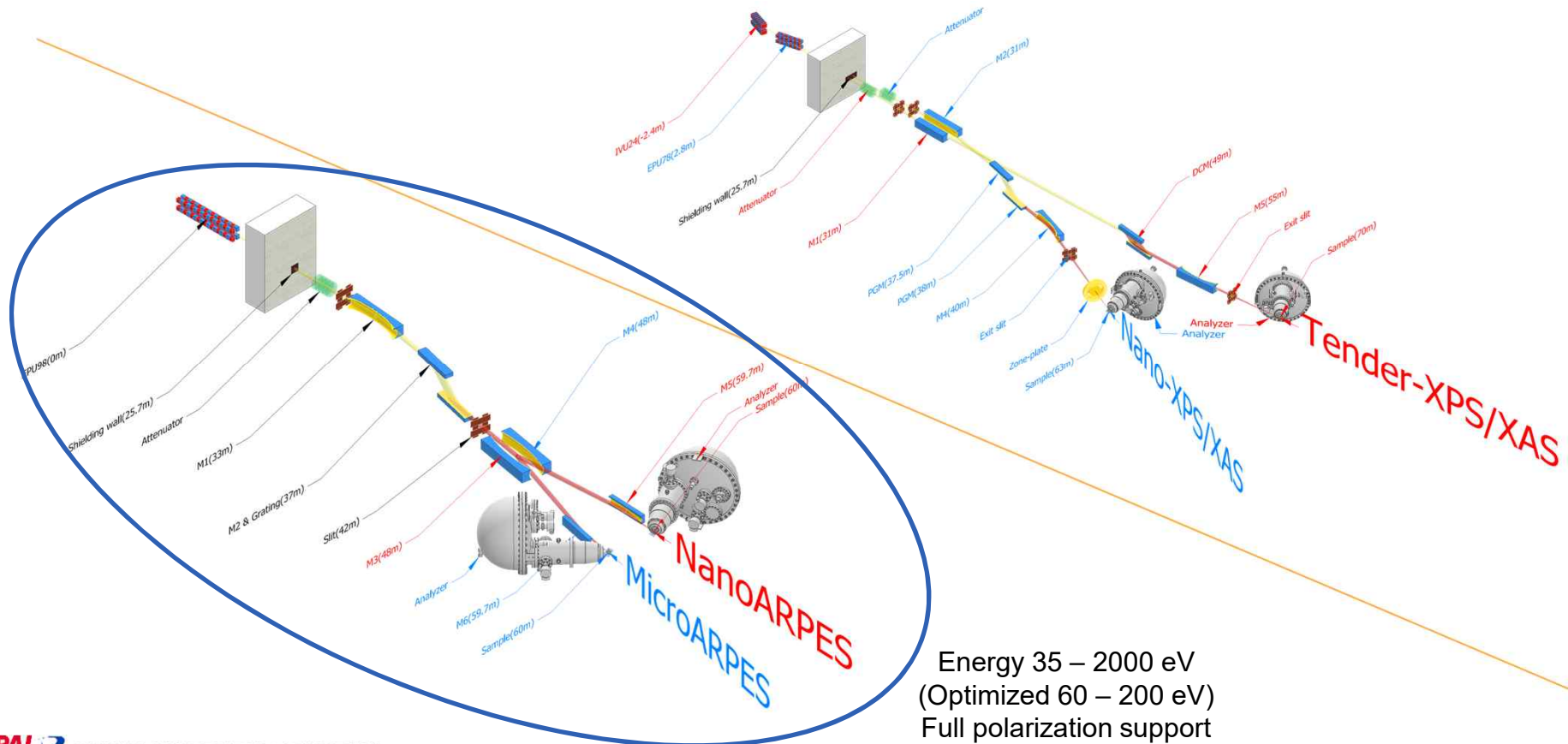
NEXAFS, **XPS**

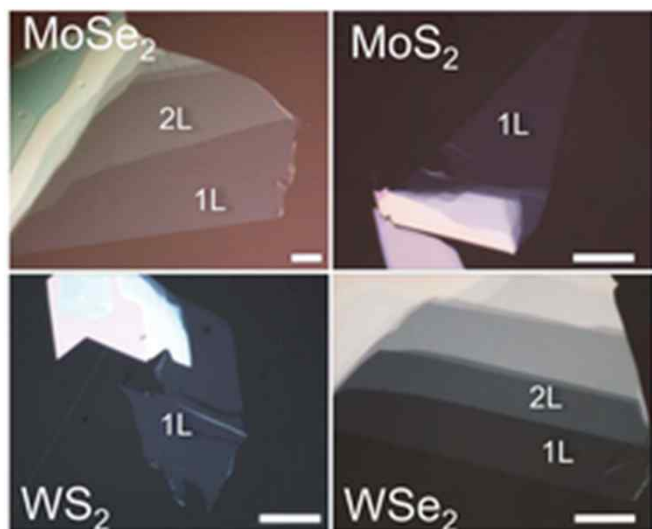
XMCD, XMLD

STXM, cryo-ptychography

nanoARPES beamline

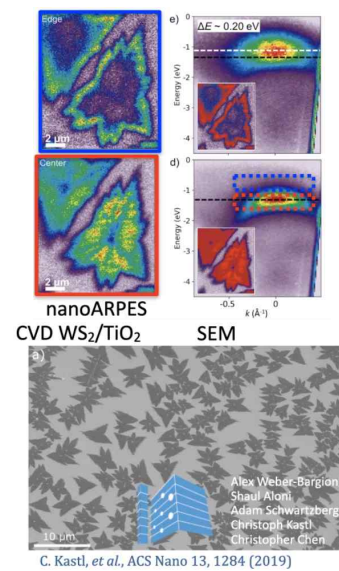
Layout overviews of Soft X-ray beamlines



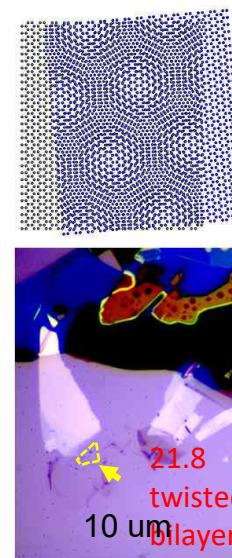


Thickness variation of vdW materials Bar: 10 μm

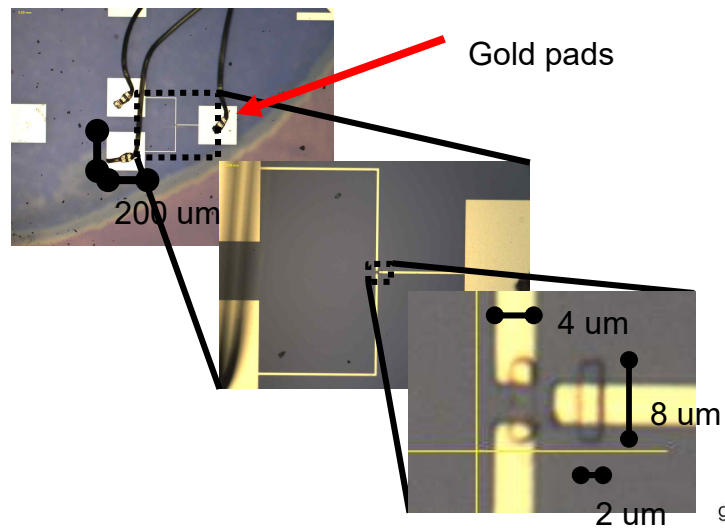
Adv. Mater. 31, 25 (2019)



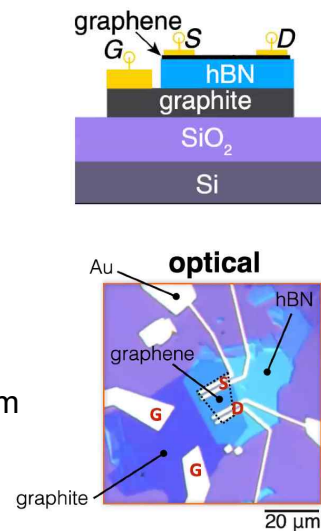
Spatial deviation



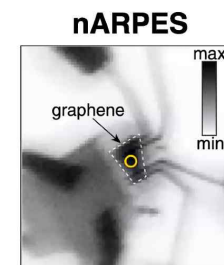
“Magically” stacked multi layers



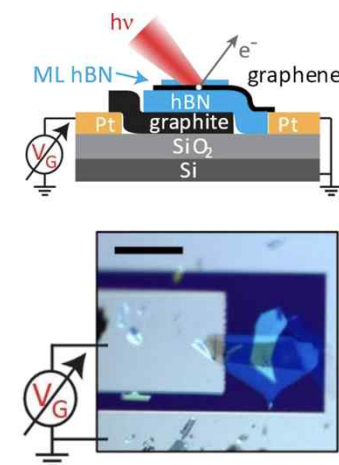
VO₂, Pre-programmed (VO_{2±x})
neuromorphic devices



R. Muzzio, *et al.*, Phys. Rev. B 101, 201409(R), (2020)

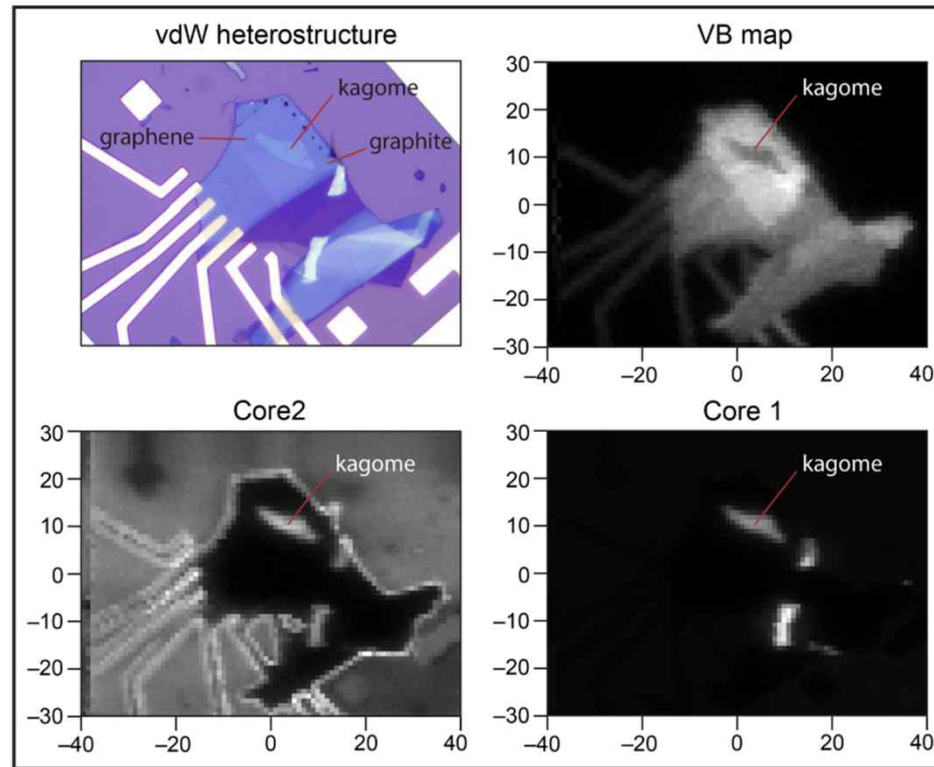


Gating devices

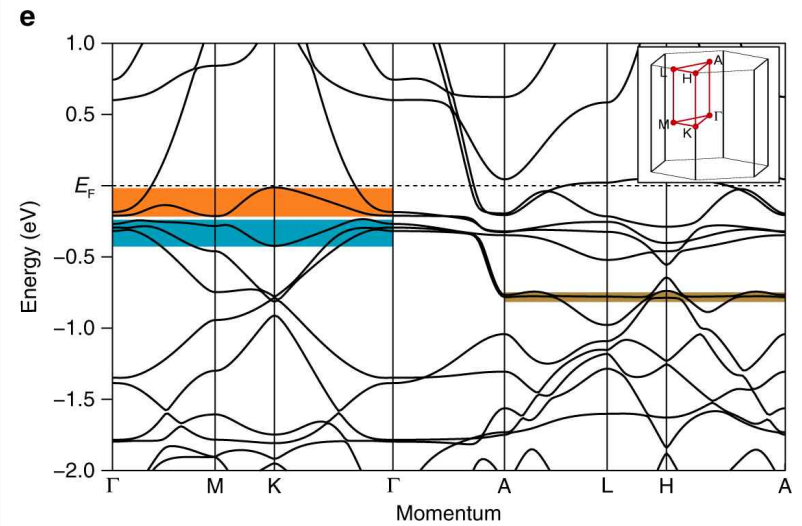


Nature 572, 220 (2019)

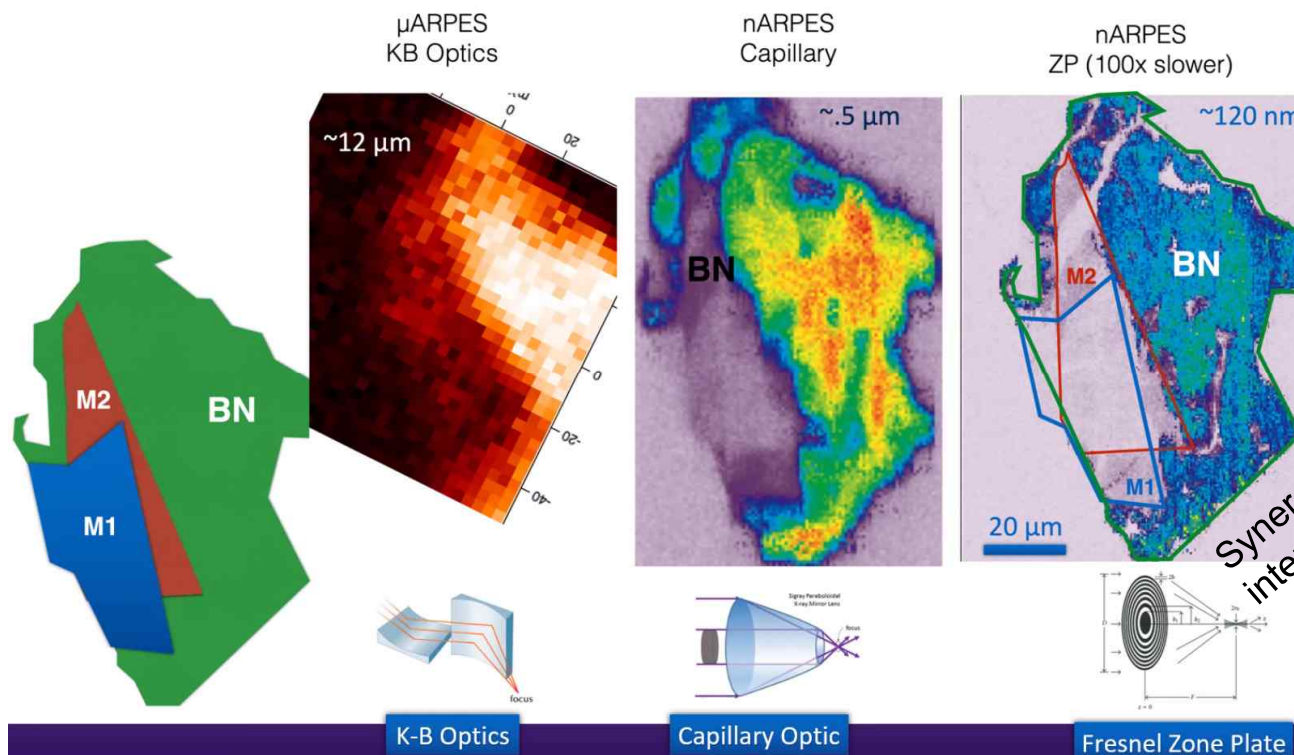
Eli Rotenberg (and Sae Hee Ryu), ALS MAESTRO



Mingu Kang, SNU, taken at MAESTRO



Few-layer Kagome gating device
controlling flat band energy



Synergetic with stronger intensity and coherency of 4GSR!

Eli Rotenberg, ALS MAESTRO

Target specifications – nanoARPES beamline

nanoARPES branch

Spot size: 1 μm (100 nm)

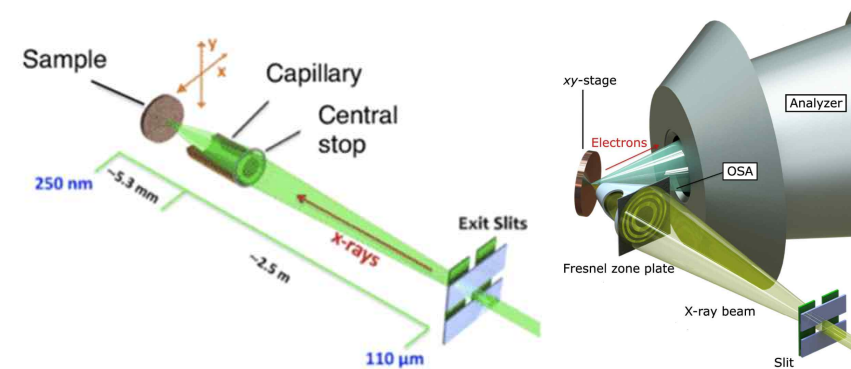
Targets: small single crystals

Exfoliated few layers

Moire superlattices and heterostructures

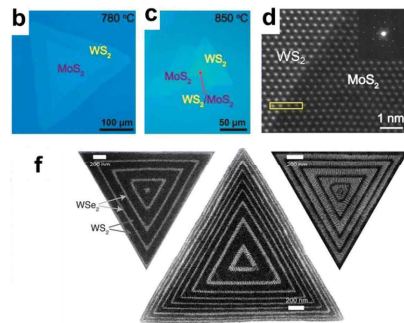
In-operando devices (gating, strain)

**Spatial resolution, stability and repeatability,
fine control over beam alignment and scanning**

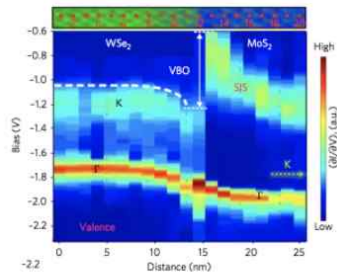


X-ray Optics	Fresnel ZP	KB Mirrors	Sigray
ZP-equivalent Numerical Aperture (based on outermost zone; smaller is better)	30 nm	16 nm	4 nm
Achievable Focus Resolution (Typical Value Best Possible)	Very High (200 nm 10 nm)	Very High (1 μm 20 nm)	High (1-2 μm 200 nm)
Handling/Ease of Alignment (Compact)	✓	✗	✓
Achromatic	✗	✓	✓
Working Distance Range Selection	1 mm – 30 mm	10 cm – 10's m	1 – 200 mm
Efficiency	~10%	~75%	>85% (single-bounce)
In-line with Beam	✓	✗	✓
Price (including beamline costs & motion control systems)	High	Mid to High (long beamline & stability needs)	Mid

Lateral hetero structure

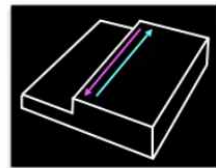


B. Kundu, Emergent Mater. 2021

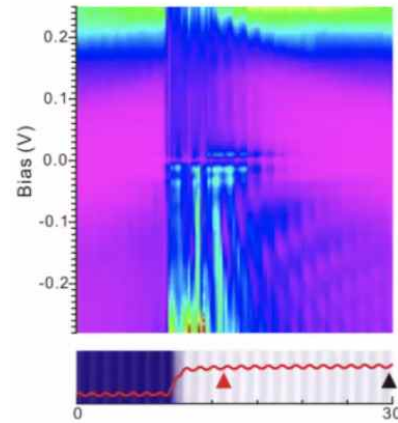


C. Zhang, Nat. NanoTech. 2018

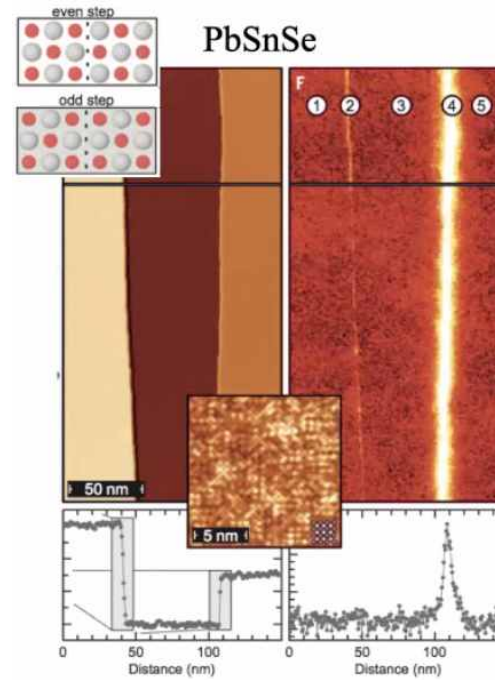
Topological edge state



ZrTe₅



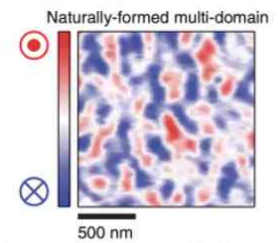
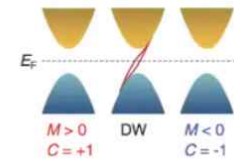
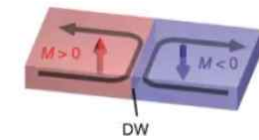
X.-B. Li, PRL 2016



P. Sessi, Science 2016

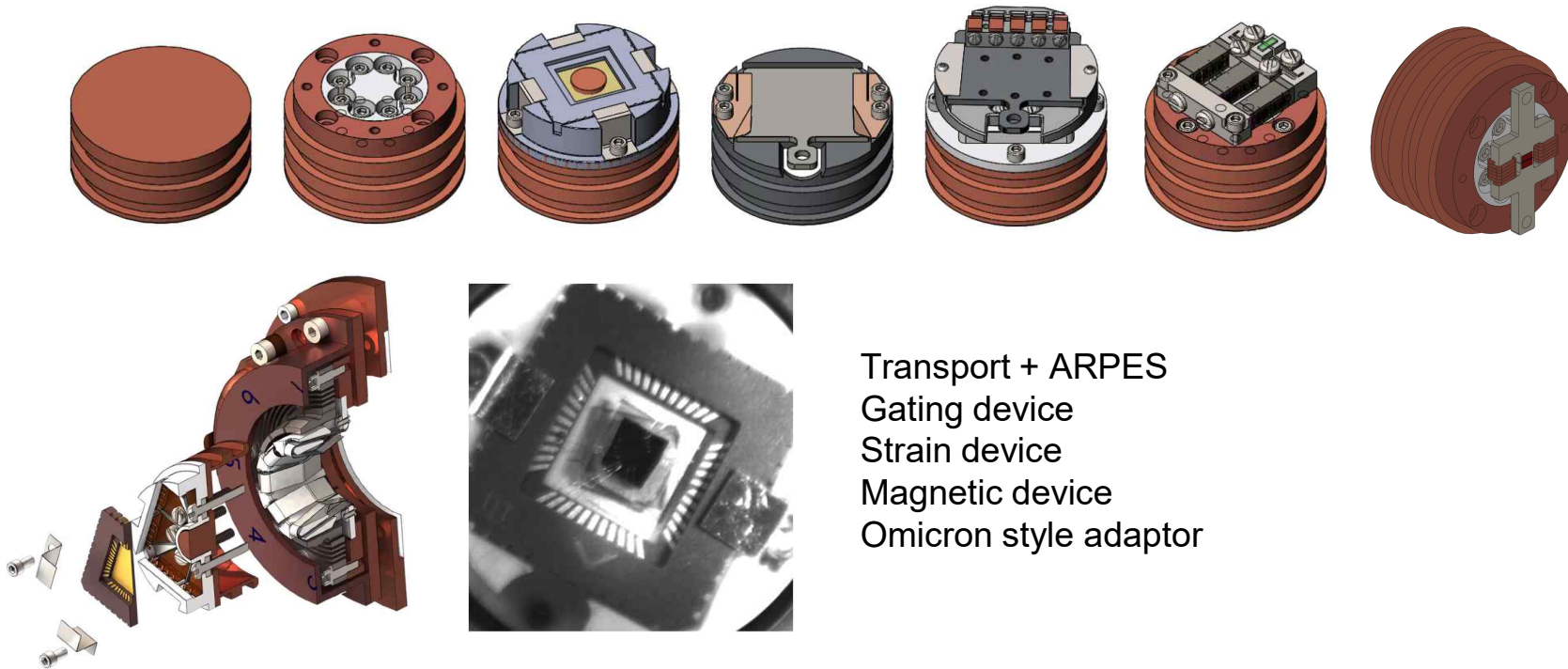
Domain wall

Mag-TI



K. Yasuda, Science 2017

In-operando measurement



Target specifications – nanoARPES beamline

nanoARPES beamline

nanoARPES branch

Spot size: 1 μm (100 nm)

Targets: small single crystals

Exfoliated few layers

Moire superlattices and heterostructures

In-operando devices (gating, strain)

**Spatial resolution, stability and repeatability,
fine control over beam alignment and scanning**

microARPES branch

Spot size: 10 μm

Targets: Large-domain crystals

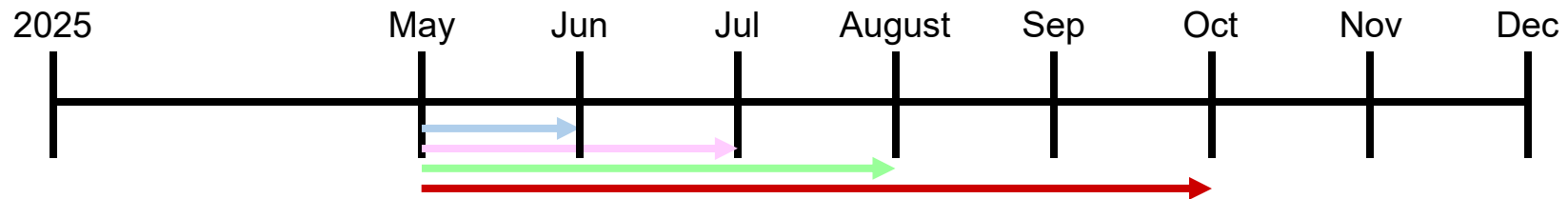
Standard thin films

Bulk crystals

In-operando devices (magnetic field, dosing)

**High photon flux, excellent energy resolution,
simplified, user friendly operation.**

Plan



→ Thermal study on M1/grating depending on M1 grazing angle

→ Comparison of gratings with each C_{ff} in terms of flux and energy resolution

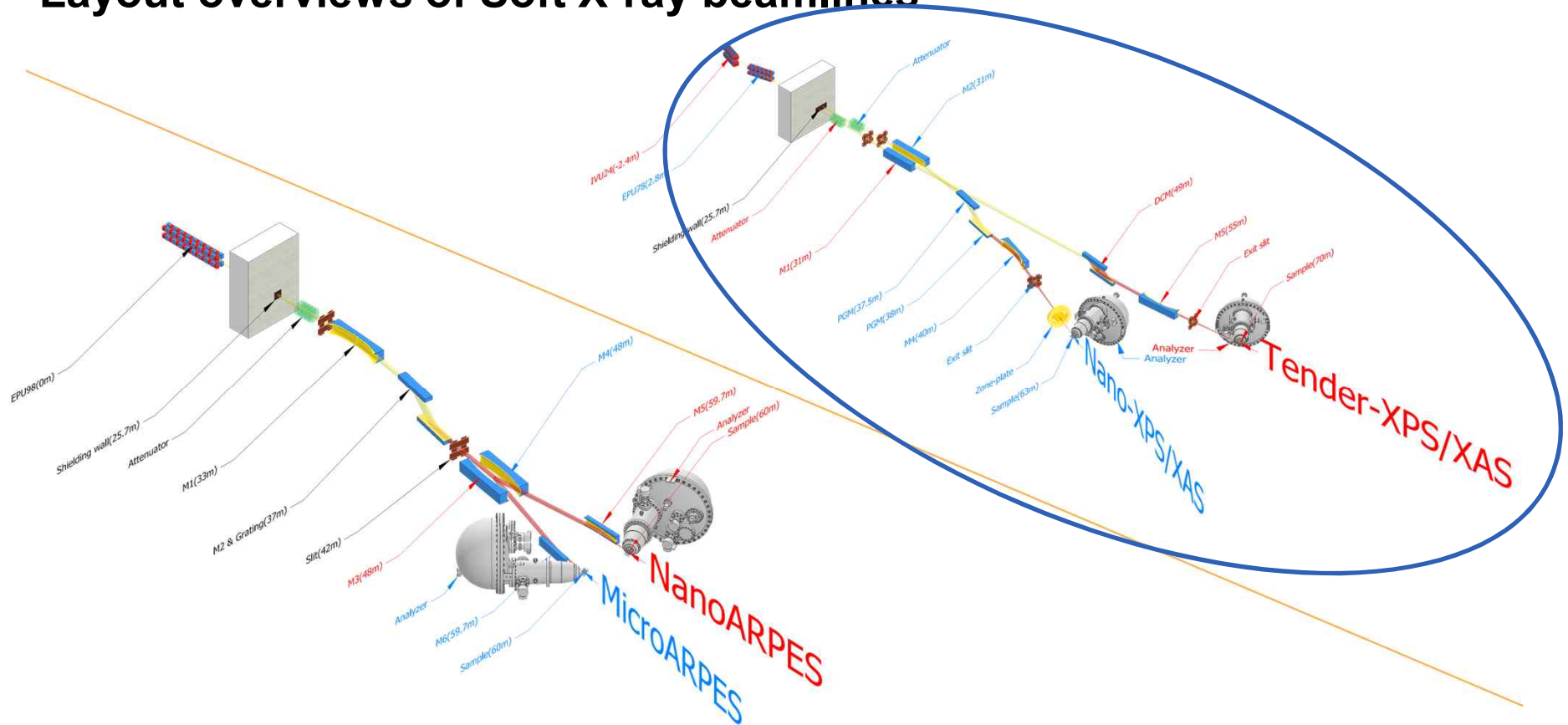
→ Extrinsic effects (thermal, errors, etc.) on the energy, spatial resolution, and flux

-> Curves of (Spot size)/(flux)/(energy resolution) on photon energy

→ Optimizing layout (~ Oct)

(Start designing endstations)

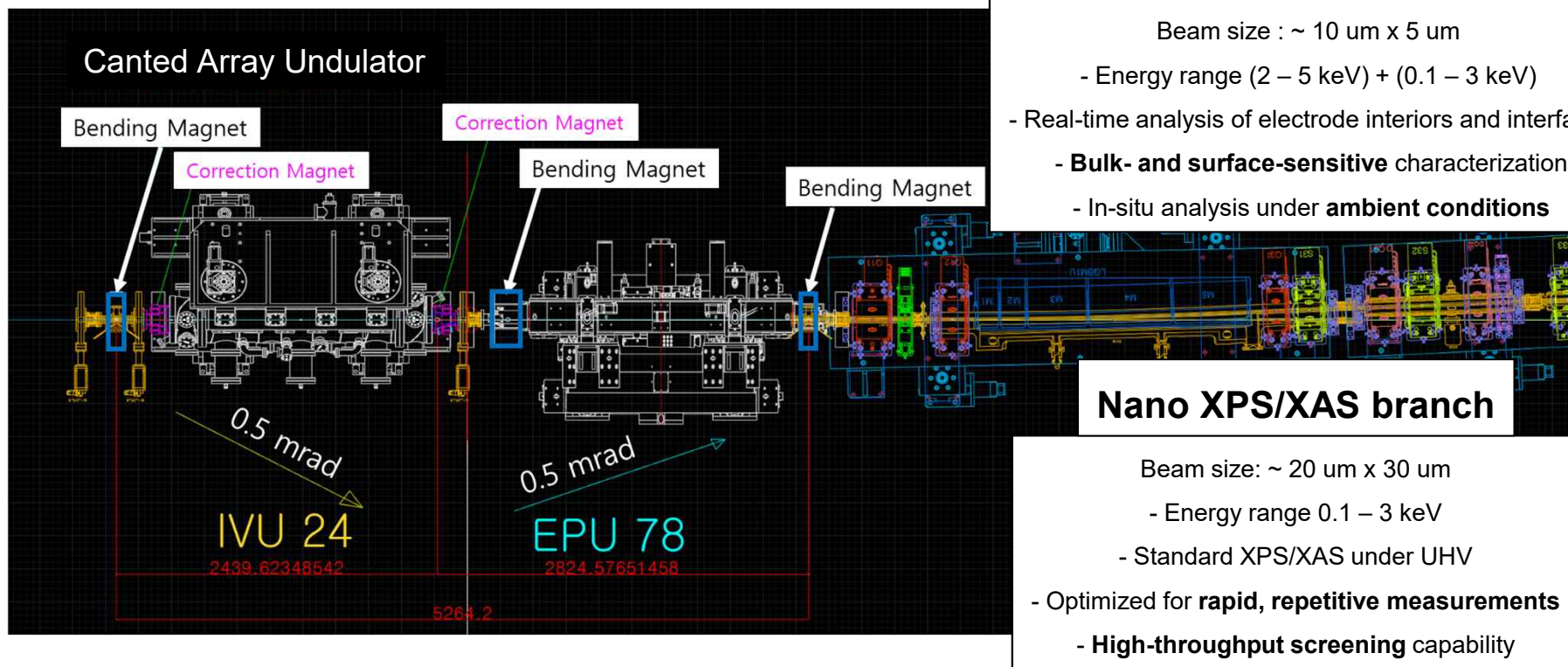
Layout overviews of Soft X-ray beamlines

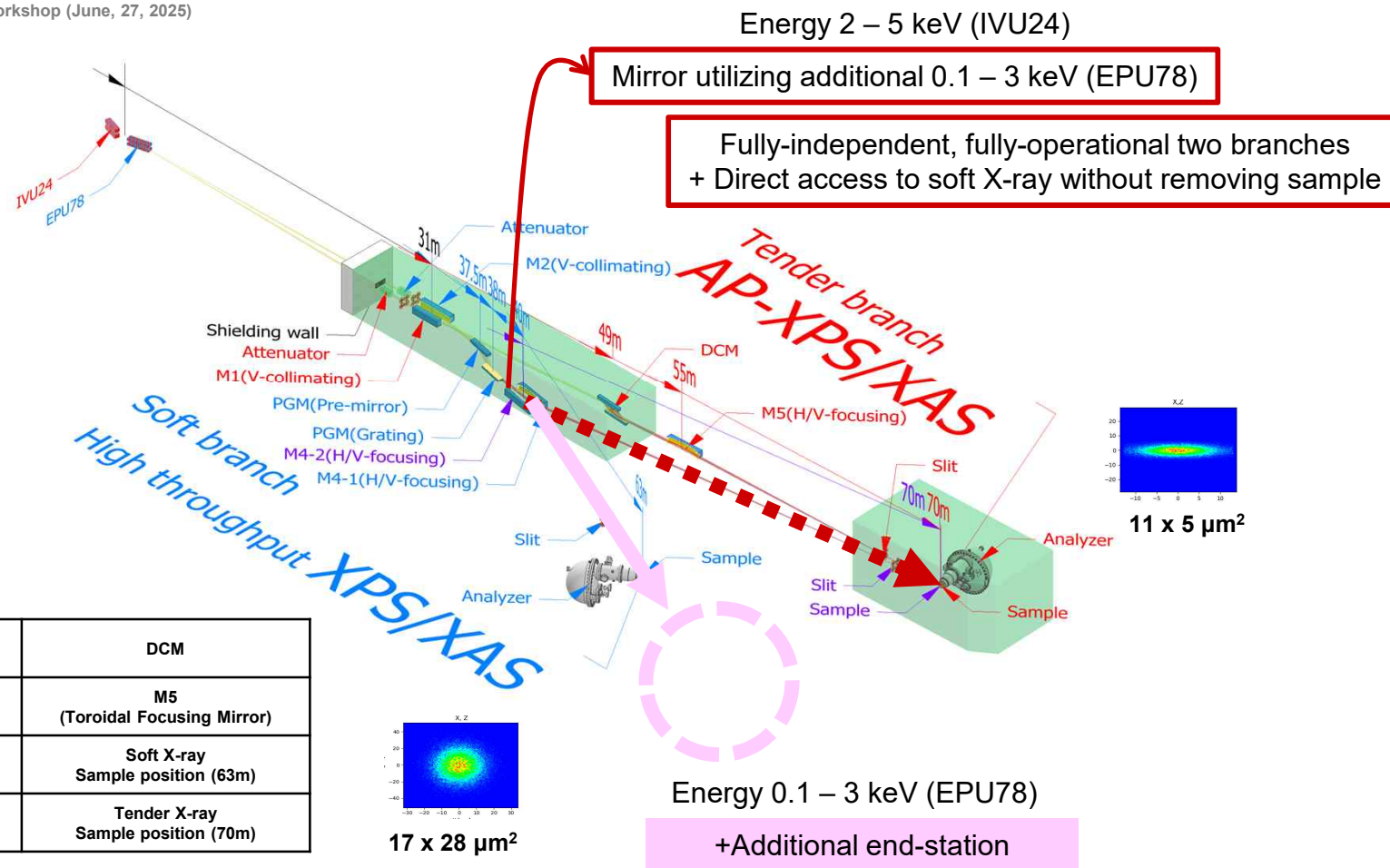


Soft X-ray Nanoprobe beamline

ID26 Soft X-ray NanoProbe beamline goal

Photon Source	EPU78(L=2m)	IVU24(L=1.5m)
Energy range	90 - 3200 eV	2000 - 5000eV
Resolution	5000 - 10000	>10000(at 4keV)
Beam size at Sample	14um x 36um	5.7um x 12.6um
Photon Flux [ph/s/0.1%B.W.]	6.3×10^{14}	1.59×10^{15}
Brilliance [photons.s-1 mrad -1. mm- 2(0.1%B.W)]	6.8×10^{18} at 15mm gap	1×10^{21} at 5mm gap

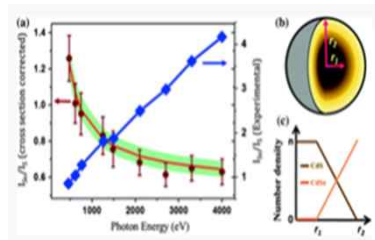




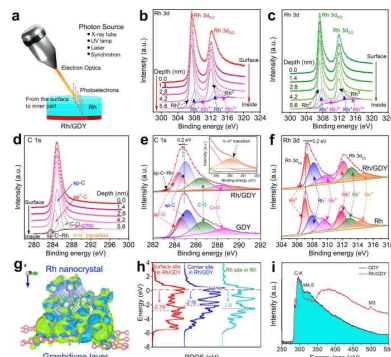
M1 & M2 (Vertical Collimating Mirror)	DCM
M3 Reflection mirror	M5 (Toroidal Focusing Mirror)
PGM	Soft X-ray Sample position (63m)
M4 (Toroidal Focusing Mirror)	Tender X-ray Sample position (70m)

❖ Tender AP-XPS/XAS

- Tender Energy [2 ~ 5keV (+ 0.1 ~ 3 keV)]
- Tender Ambient Pressure XPS
- Tender Ambient Pressure XAS

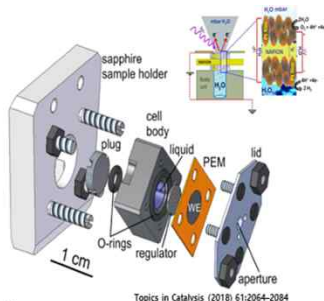


energy-dependent depth resolution



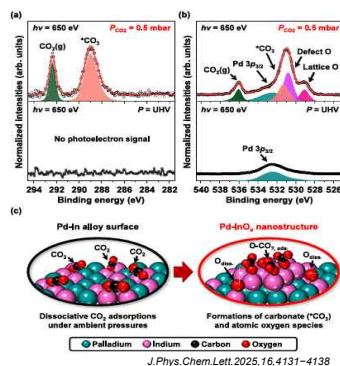
Nature Communications volume 13, Article number: 5227 (2022)

depth profiling experiments



Topics in Catalysis (2018) 61:2064–2084

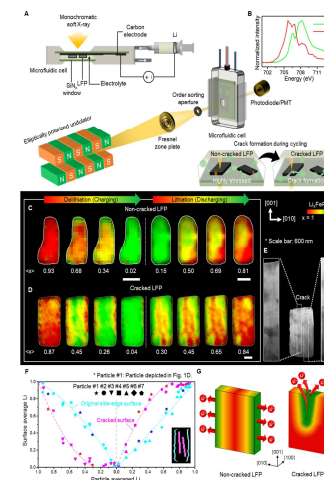
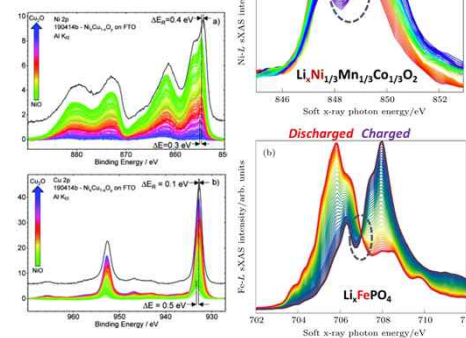
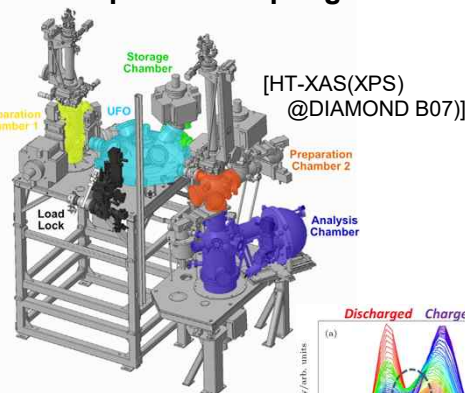
Electro chemical



CO₂ Conversion

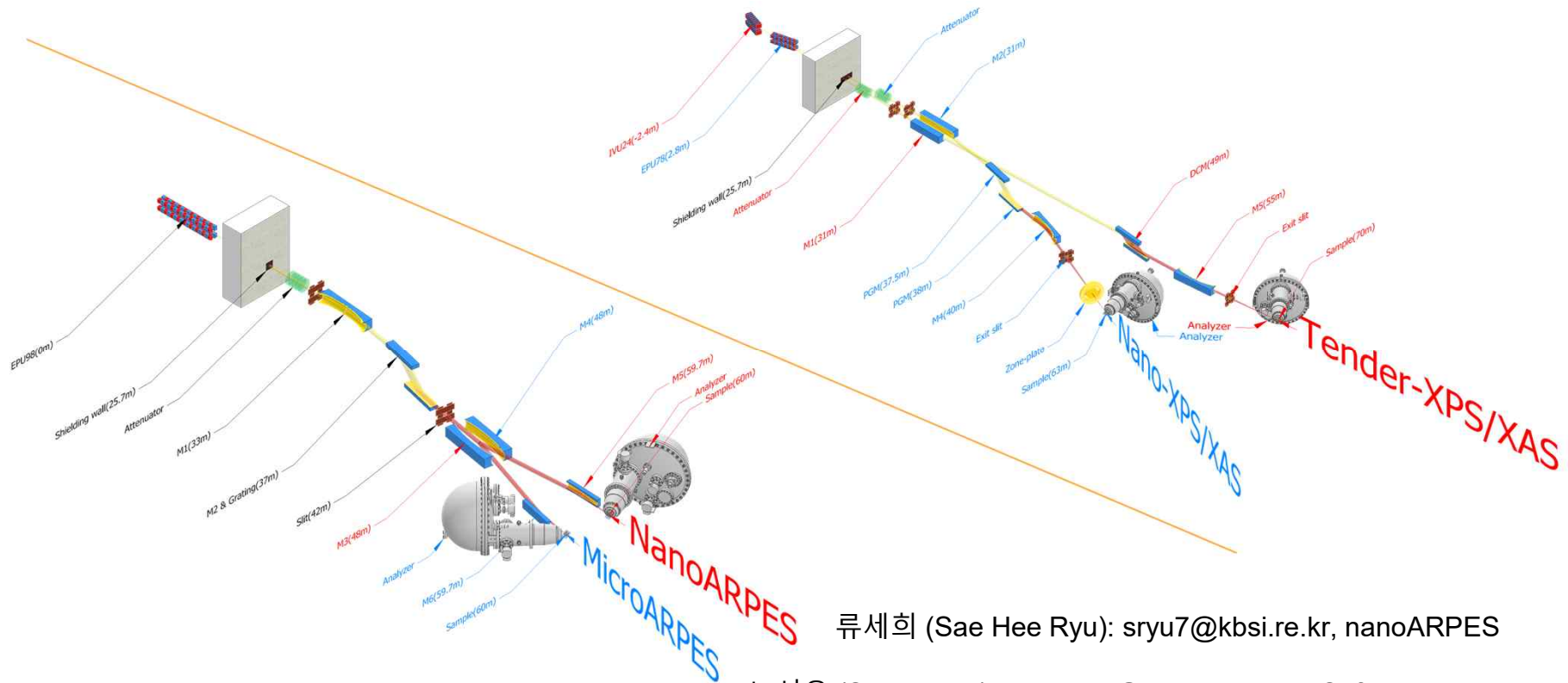
❖ Nano-XPS/XAS

- Soft Energy (0.1 ~ 3 keV)
- High-throughput XAS(XPS)
- Beam focusing(optional) to sub-micron size
- Automated sample measurement
- Open to accepting a candidate systems



Supplementary

Contacts for Soft X-ray beamlines



류세희 (Sae Hee Ryu): sryu7@kbsi.re.kr, nanoARPES

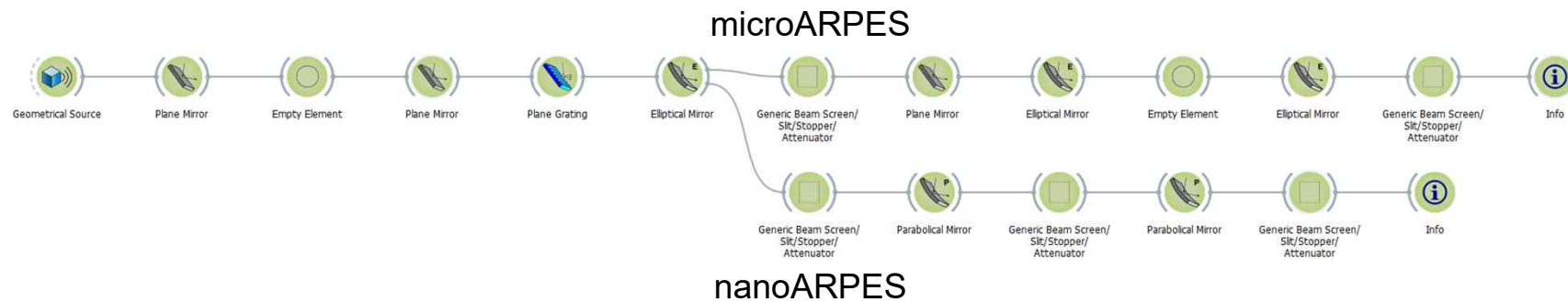
노시우 (Siwoo Noh): nsw0809@postech.ac.kr, Soft X-ray Nanoprobe

Target specifications – nanoARPES beamline

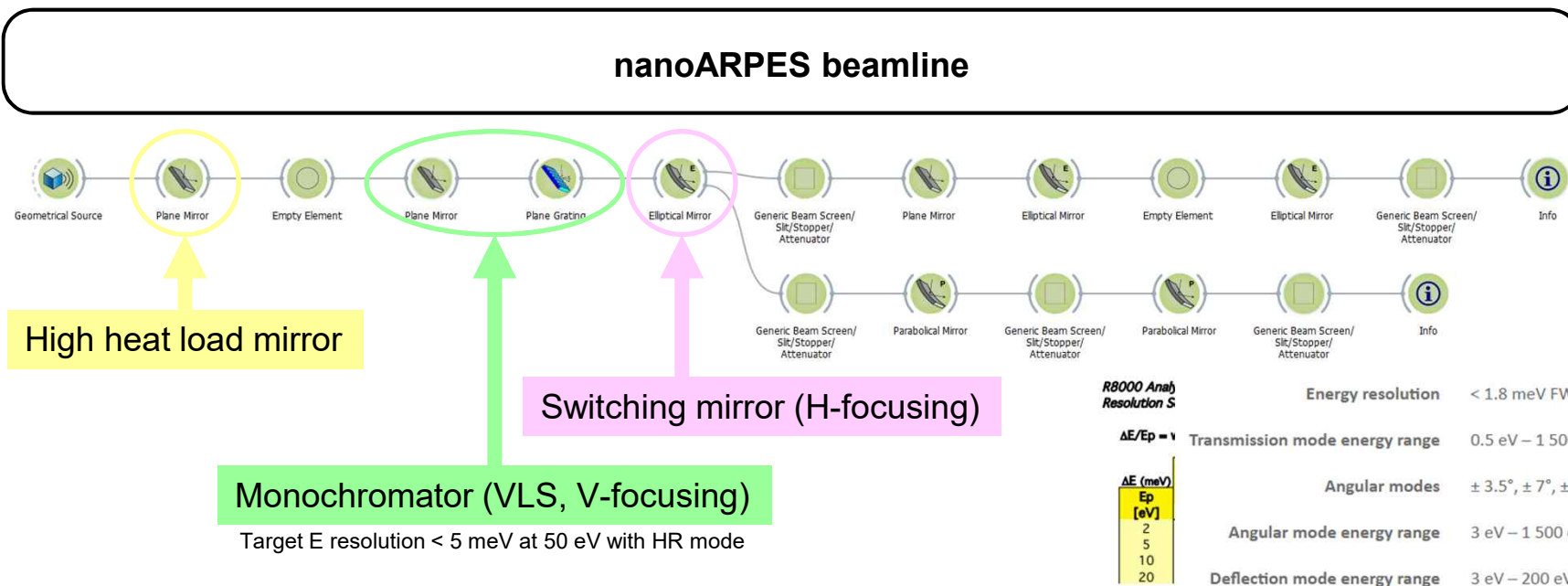
nanoARPES beamline

Beamline design philosophy

1. Minimizing complexity: VLS grating, tangential-only focusing
2. Optimizing for low energies (60 – 200 eV)
3. Two track strategy: high flux, and high resolution gratings



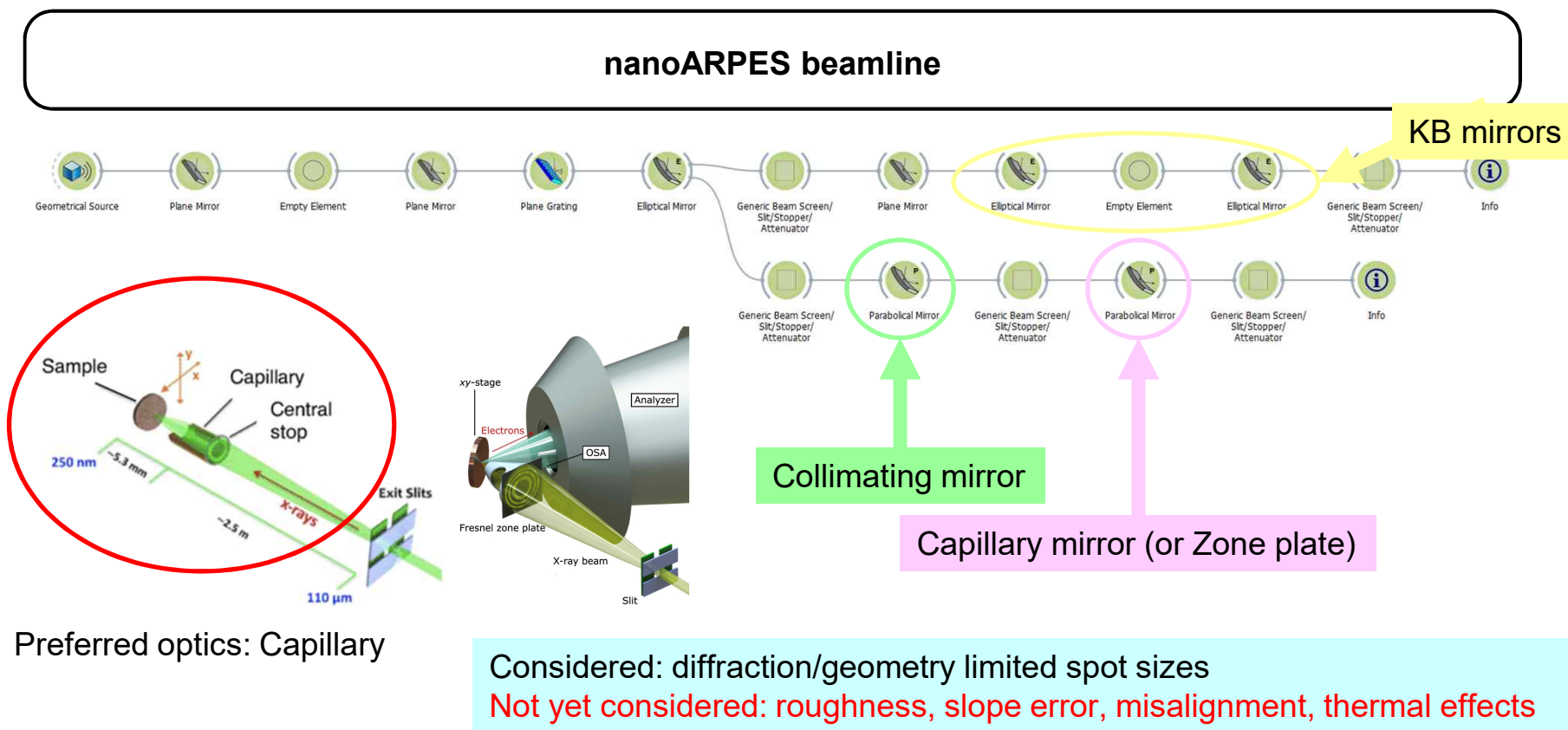
Target specifications – nanoARPES beamline



High grazing angle -> higher harmonics rejection, comparatively higher energy resolution, **lower overall flux**
 Low grazing angle -> overall higher flux, **higher heat load to grating (bad for energy resolution)**

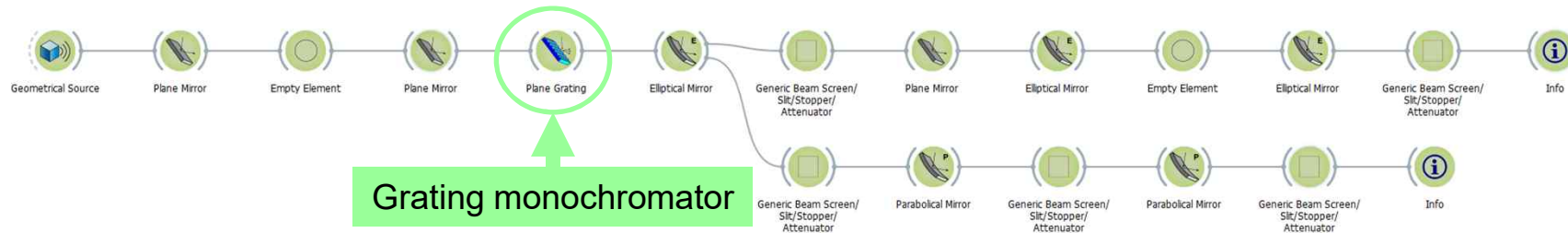
Higher C_{ff} grating -> Overfill downstream optics, smaller diffraction limited spot size, **shorter energy range of optimized grating efficiency (bad for energy scan)**
 Low C_{ff} grating -> Underfill downstream optics, longer range of optimized grating efficiency, **bigger diffraction limited spot size**

Target specifications – nanoARPES beamline



Monochromator optimizations

nanoARPES beamline



Grating monochromator

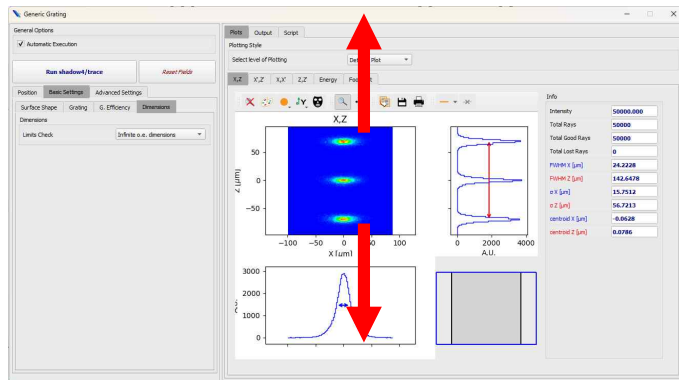
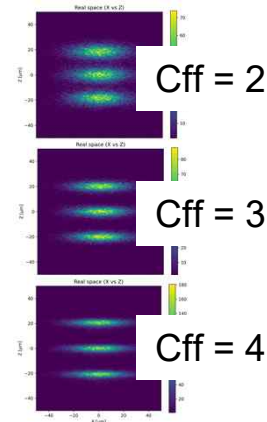


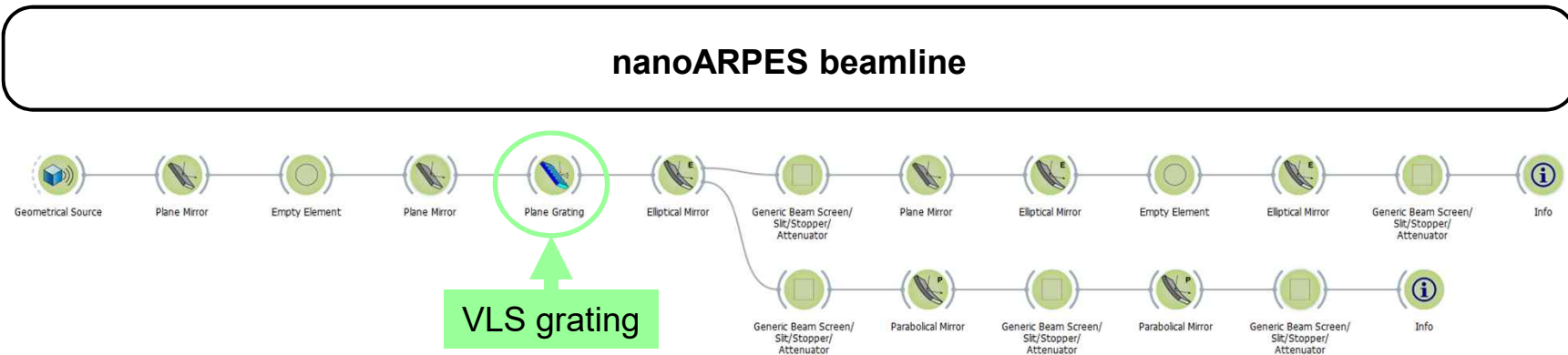
Image at the slit



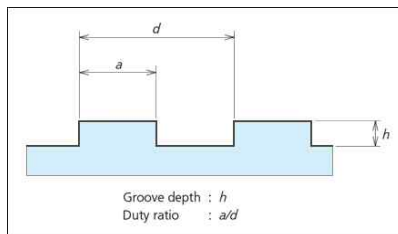
$$\frac{d\theta_{\text{diff}}}{d\lambda} = \frac{n}{d \cdot \cos \theta_{\text{diff}}} \quad d : \text{pitch of groove}$$

1. Angular separation (grating density)
2. Intermediate beam spot size (Cff, magnification, diffraction)

Target specifications – nanoARPES beamline

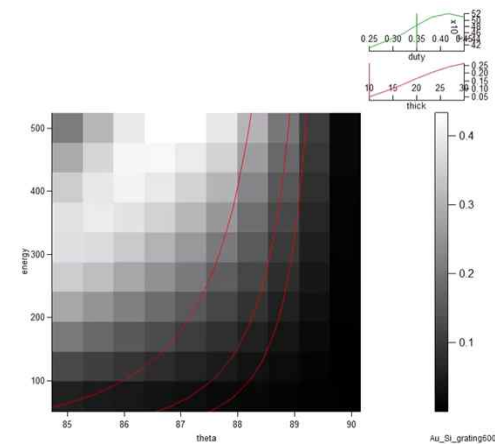
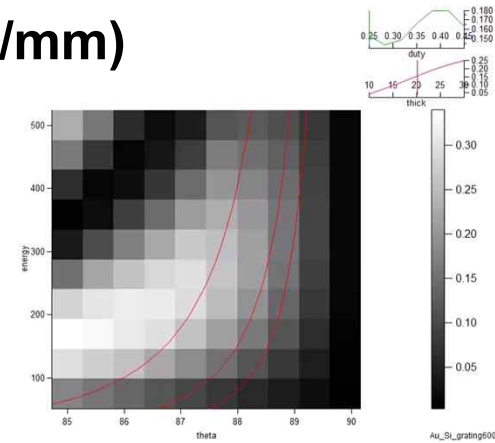
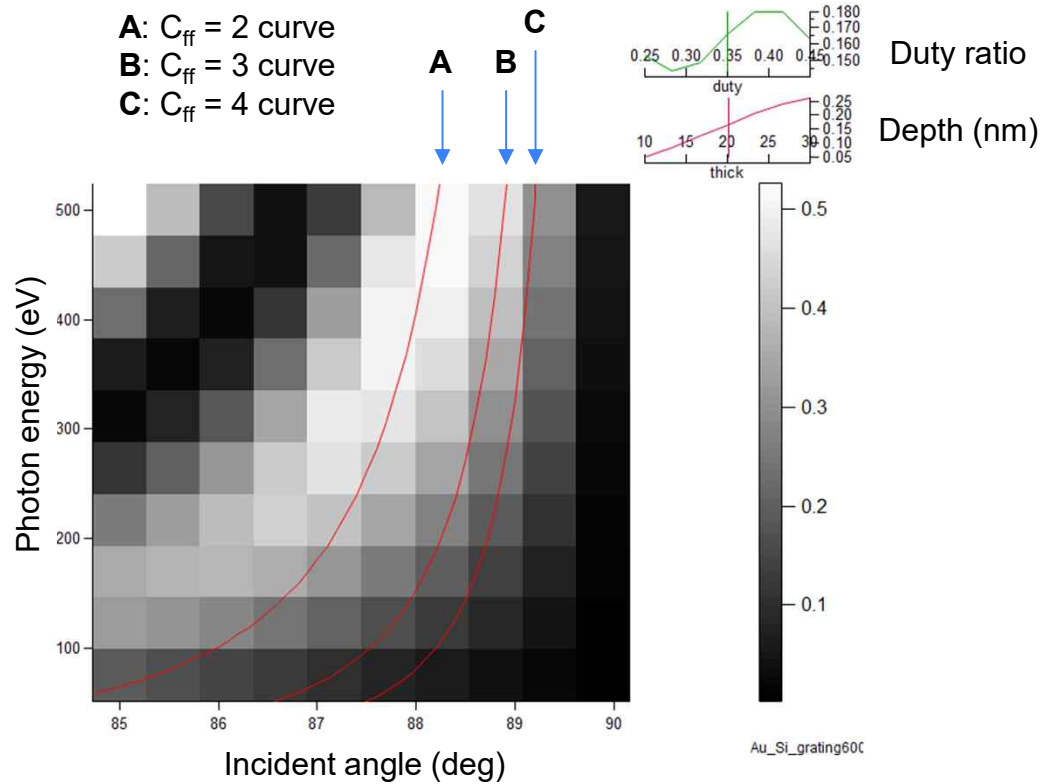


Grating parameters

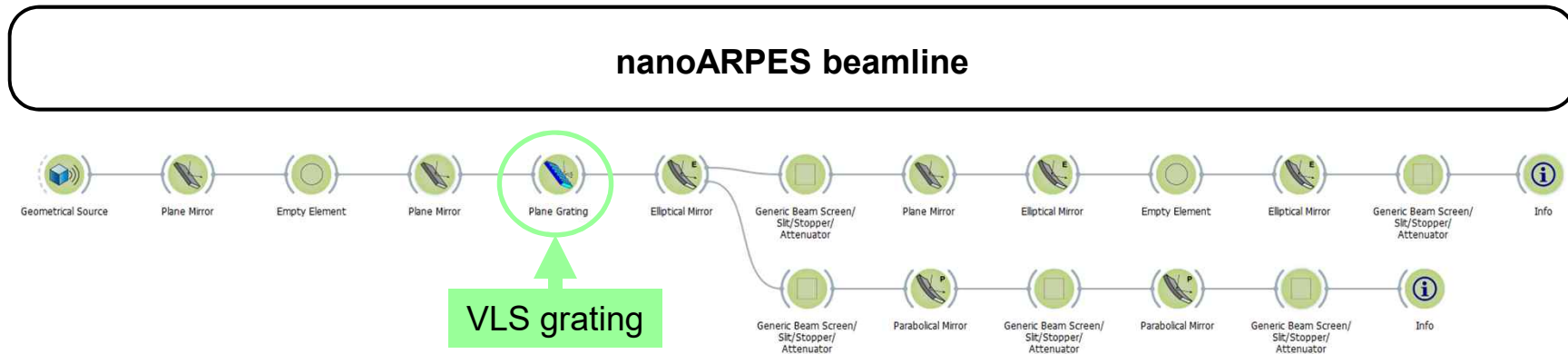


Optimization needed for higher throughput over target energies.

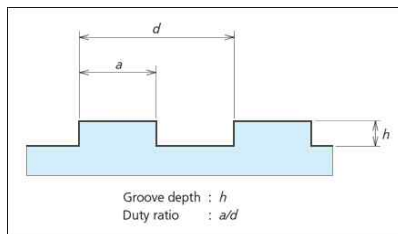
Grating efficiency optimization (e. g. 600 l/mm)



Target specifications – nanoARPES beamline

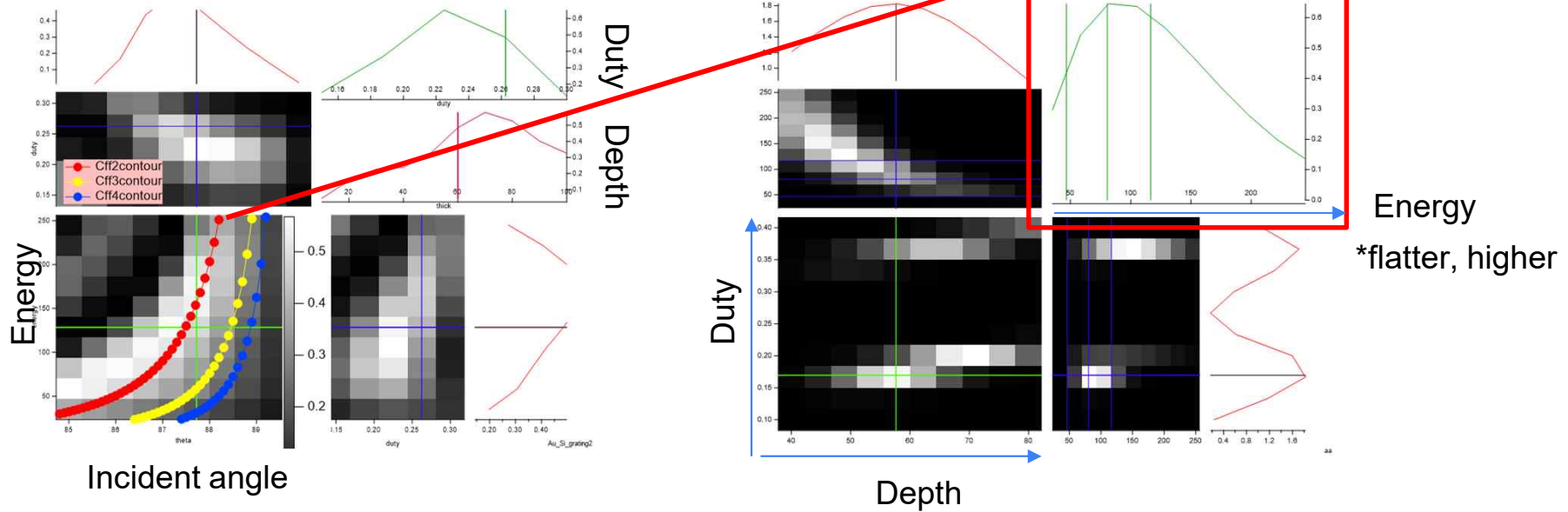


Grating parameters



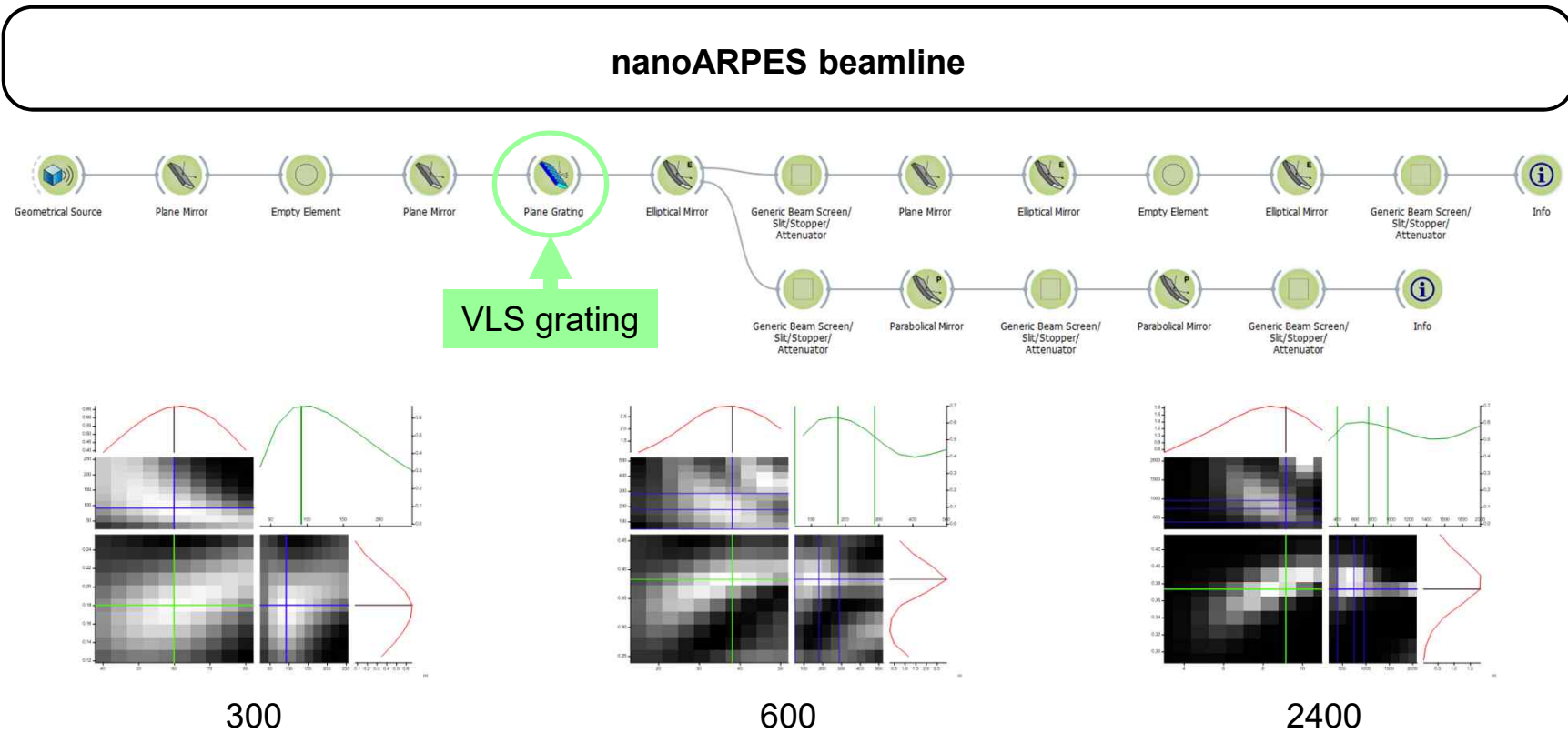
Grating density (l/mm)	E_{\min} (eV)	E_{\max} (eV)	C_{ff}	Depth (nm)	Duty
300	35	250	2.2	60	0.18
600	70	500	2.2	38	0.38
2400	280	2000	2.2	9	0.37

4D intensity plot of Efficiency (Incident angle, energy, depth, duty)



New plot! Efficiency (depth, duty, energy) along the $Cff \approx 2$ (actually 2.2) curve
Easier to decide which pattern to use

Target specifications – nanoARPES beamline



MAC comments for Soft X-ray NanoProbe BL

Optimization of the Soft X-ray NanoProbe Beamline as a Canted Beamline

- The optimization of the beamline as a canted beamline, allowing both the Tender XPS/XAS and Nano XPS/XAS branch beamlines to be utilized 100%, is highly welcomed.
- Considering the beamline space and thermal load management, this optimization is acceptable.
- The independent beamline may provide better opportunities for scientific applications.

Further Applications and Scientific Strategy for the Elliptically Polarized Undulator (EPU) 78

- This beamline is proposed as one of the priority support beamlines for industrial use, with XPS and XAS as the primary experimental methods.
- Our primary goal is to meet this requirement. Looking to the future, we anticipate increased demand for quantum materials analysis. Polarized photons from the EPU 78 will be fundamental in measuring magnetic properties and expanding the range of scientific applications.

Introduction of an Angle-Resolved Electron Analyzer for the Tender AP-XPS/XAS System

- The basic requirements are satisfied with the current design.
- The development of an angle-resolved electron analyzer for ambient pressure environments is ongoing. We will monitor its progress and, if the analyzer's performance is sufficient, explore the possibility of introducing it.

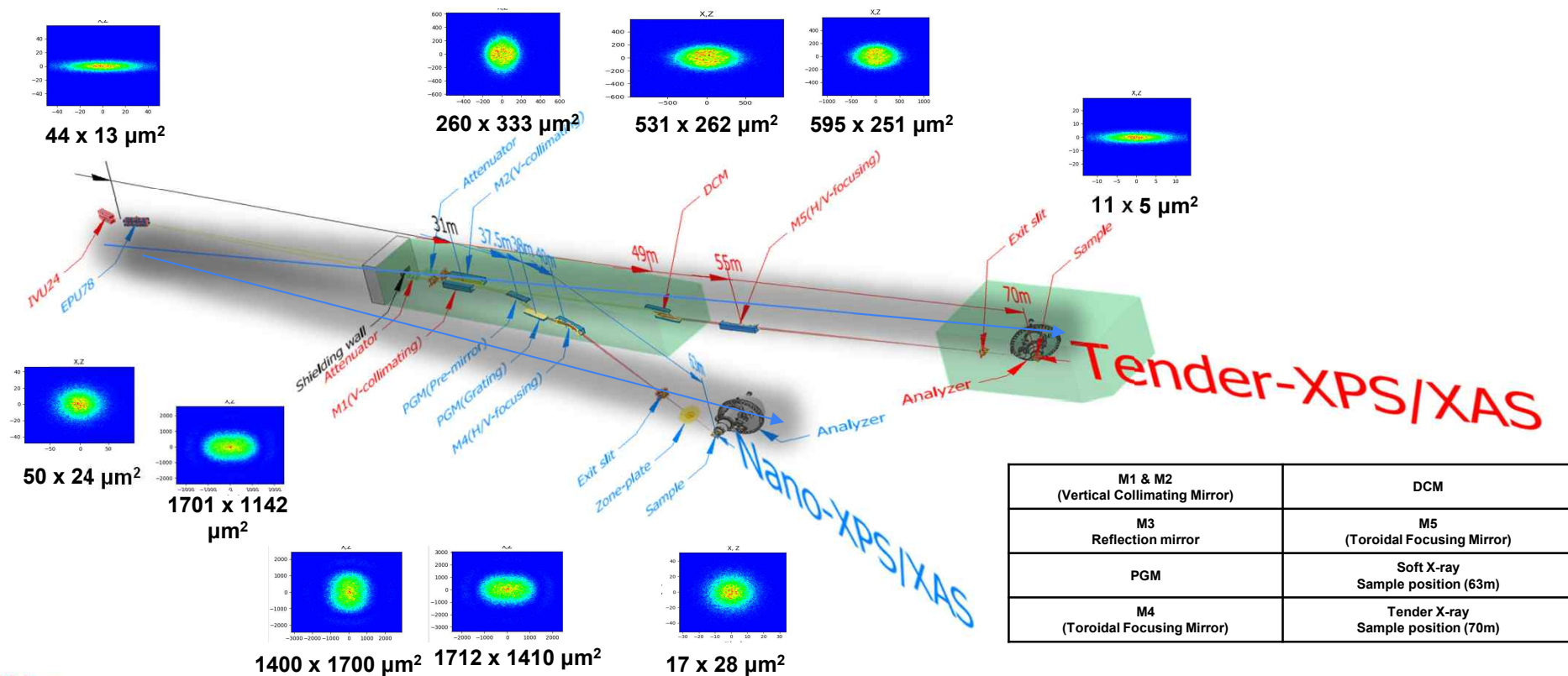
Enhancement of Unique Properties for Microscopy and Spectroscopy Experiments

- The NanoXPS/XAS beamline will be optimized to support both microscopy and spectroscopy experiments.

Utilization of the Full Range of Photon Energy

- Currently, this beamline is designed as two independent beamlines.
- It is possible to merge these two beamlines into a single tender (or soft) end station to utilize the full photon energy range from 100 to 5000 eV by introducing an additional refocusing mirror system. Future improvements will be considered in the beamline design.

ID26 Soft X-ray NanoProbe BL Layout



Applicable techniques(Tender AP-XPS beamline)



In-situ are feasible at the 4GSR ID26 beamline

- ID26 supports the tender X-ray range (2-5 KeV)
- High-flux, high-stability beamline equipped with DCM optics ideal for in situ spectroscopy
- Compatible with three-electrode flow cell setups for liquid–solid interface studies
- potential, and temperature controllable

phosphorus chemistry, and operando electrochemistry



This article is licensed under CC-BY 4.0

Open Access

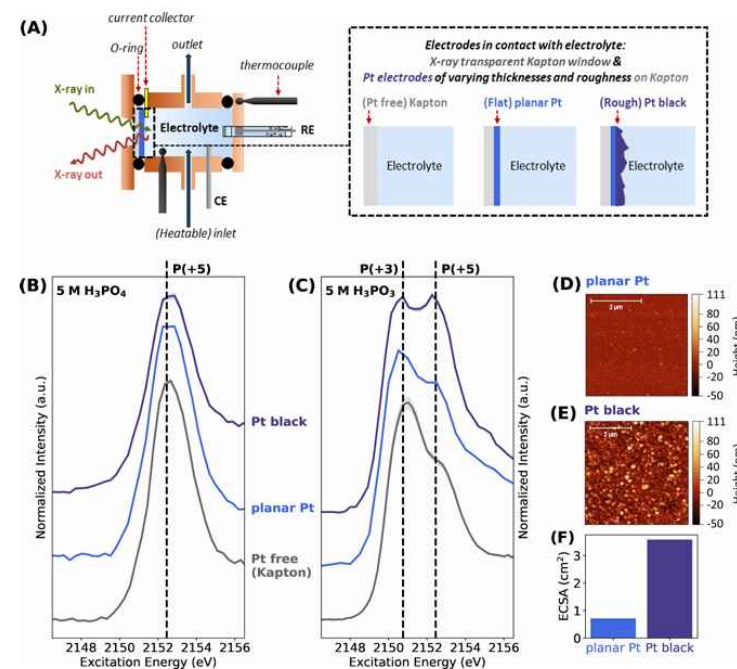
Article

Elucidating the Complex Oxidation Behavior of Aqueous H_3PO_3 on Pt Electrodes via *In Situ* Tender X-ray Absorption Near-Edge Structure Spectroscopy at the P K-Edge

Romualdus Enggar Wibowo,* Raul Garcia-Diez, Tomas Bystron, Marianne van der Merwe, Martin Prokop, Mauricio D. Arce, Anna Efimenko, Alexander Steigert, Milan Bernauer, Regan G. Wilks, Karel Bouzek, and Marcus Bär*

Cite This: *J. Am. Chem. Soc.* 2024, 146, 7386–7399

Read Online



J. Am. Chem. Soc. 2024, 146, 7386–7399

Applicable techniques(Tender AP-XPS beamline)



THE JOURNAL OF
PHYSICAL
CHEMISTRY
A JOURNAL OF THE AMERICAN CHEMICAL SOCIETY
pubs.acs.org/JPC

This article is licensed under CC-BY 4.0

Article

Operando Characterization of Electrochemistry at the Rutile $\text{TiO}_2(110)/0.1 \text{ M HCl}$ Interface Using Ambient Pressure XPS

Jiangdong Yu, Conor Byrne, Jameel Imran, Zoë Henderson, Katherine B. Holt, Alexander I. Large, Georg Held, Alex Walton,* and Geoff Thornton*

Cite This: *J. Phys. Chem. C* 2024, 128, 20933–20939

Read Online

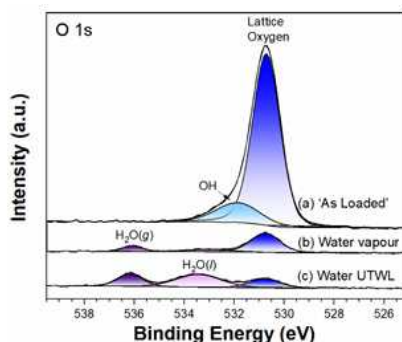


Figure 3. O 1s AP-XPS ($h\nu = 1487 \text{ eV}$) from $\text{TiO}_2(110)$ for (a) as-loaded, (b) water vapor, and (c) water UTWL. The fits to Voigt peak shapes along with the Shirley backgrounds are shown.

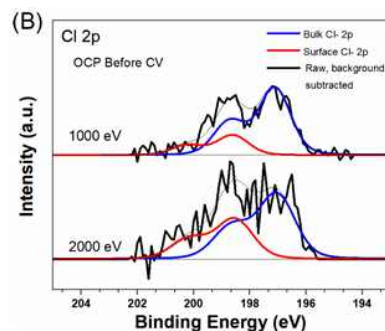


Figure 8. (A) Cl 2p AP-XPS ($h\nu = 1487 \text{ eV}$) from $\text{TiO}_2(110)/0.1 \text{ M HCl}$ before CVs and after CVs at different potential biases: (a) OCP before CV, (b) +2.8 V, (c) +0.3 V, and (d) OCP; (B) photon depth profiling at 1000 and 2000 eV, where spectra are normalized to the bulk (aqueous) Cl $2p_{3/2}$ peak. The fits to Voigt peak shapes are shown along with the Shirley backgrounds in (A).

Under operando potential control, photon energy-tuned AP-XPS enabled non-destructive depth-resolved analysis of Cl^- species at the $\text{TiO}_2/\text{electrolyte}$ interface.

- Real-time adsorption/desorption of Cl^- ions was observed under **operando** conditions, which can be applied to interface reaction studies at ID26.

- Photon energy tuning (AP-XPS) enabled **depth-resolved chemical analysis**, which can also be implemented at ID26 within its tender X-ray range (2–5 keV).

- Formation of C–Cl and C– Cl_2 species was detected, supporting ID26-based analysis of **solid–liquid organic/inorganic** interfacial reactions.

- The Ultrathin Water Wetting Layer (UTWL) approach enables vacuum-compatible electrochemical interface analysis, which can be implemented at ID26 for operando studies.

J. Phys. Chem. C 2024, 128, 20933–20939